2000 Heat Transfer Committee Best Paper Award

Effects of Reynolds Number and Free-Stream Turbulence on Boundary Layer Transition in a Compressor Cascade

Heinz-Adolf Schreiber

Wolfgang Steinert

German Aerospace Center (DLR),
Institute of Propulsion Technology,
51170 Köln, Germany

Bernhard Küsters

Siemens AG,
Power Generation (KWU),
45466 Mülheim a.d. Ruhr, Germany

An experimental and analytical study has been performed on the effect of Reynolds number and free-stream turbulence on boundary layer transition location on the suction surface of a controlled diffusion airfoil (CDA). The experiments were conducted in a rectilinear cascade facility at Reynolds numbers between 0.7 and 3.0×10^6 and turbulence intensities from about 0.7 to 4 percent. An oil streak technique and liquid crystal coatings were used to visualize the boundary layer state. For small turbulence levels and all Reynolds numbers tested, the accelerated front portion of the blade is laminar and transition occurs within a laminar separation bubble shortly after the maximum velocity near 35–40 percent of chord. For high turbulence levels (Tu>3 percent) and high Reynolds numbers, the transition region moves upstream into the accelerated front portion of the CDA blade. For those conditions, the sensitivity to surface roughness increases considerably; at Tu=4 percent, bypass transition is observed near 7–10 percent of chord. Experimental results are compared to theoretical predictions using the transition model, which is implemented in the MISES code of Youngren and Drela. Overall, the results indicate that early bypass transition at high turbulence levels must alter the profile velocity distribution for compressor blades that are designed and optimized for high Reynolds numbers. [DOI: 10.1115/1.1413471]

Introduction

The aerodynamic performance of turbomachinery blading is strongly dependent on the nature of boundary layer development on the blades. The blade boundary layer is responsible for the airfoil aerodynamic efficiency and thus for the overall performance of the machine. Several previous investigations in turbomachinery test facilities have shown that, in spite of the high free-stream turbulence and the unsteady periodic wakes of the upstream blade rows, the boundary layer is laminar along the forward parts of the blade surface. This is true especially for turbine blade sections, which usually operate at low Reynolds numbers. Also the boundary layers on compressor blades are observed to be laminar in wide areas along the accelerated blade front region. Most blade designers take advantage of the laminar boundary layer on the front and set the maximum suction side velocity around 15–30 percent of blade chord. This allows high blade loading in combination with low losses. Beyond the velocity maximum, the suction surface flow is decelerated with a relatively steep gradient and then—to keep the boundary layer slightly apart from separation—decreased monotonically in strength toward the trailing edge. These ''controlled diffusion airfoils'' (CDA) are widely in use in multistage compressors.

Several experimental investigations have provided evidence of the existence of partial laminar boundary layers on compressor blades. Studies in cascade facilities with different free-stream turbulence levels and wakes, which have been produced by moving bars, showed laminar flow on the suction side and final transition within a laminar separation bubble shortly after the velocity maximum [1,2]. In real compressor environments, detailed measurements on stator blades showed extended laminar boundary layers up to 30–50 percent of blade chord. At very low Reynolds numbers, transition occurred even further downstream [3,4]. Transition is induced in rather complex modes that depend on the incoming wakes that impinge on the blade surface boundary layers, on the profile velocity distribution, and the Reynolds number. Behind the turbulent wakes so-called calmed ''laminar-like'' regions are observed, which are followed by transition either in bypass modes or in laminar separation bubbles aft of the suction side maximum. In case of separated-flow transition the separation bubble and its extension oscillates with the blade passing frequency [5]. The turbulence level between the wakes was determined by Halstead et al. [4] to be about 2.5–3 percent and within the wake region about 5.5–6 percent. All these complex transition modes are excellently described by Halstead et al. [4], or in the paper of Cumpsty et al. [6], for example.

Essential for the above-described observations is that the corresponding tests, both in cascade facilities and in compressor test rigs, have been performed at blade chord Reynolds numbers ranging from about 0.05 to 0.45×10^6. Even tests with a special Reynolds number variation did not exceed this range. Real compressors in aeroengines, however, operate at $Re=0.6–1.2\times10^6$ even at cruise altitude [7], and industrial compressors or compressors in heavy-duty gas turbines have blade chord Reynolds numbers roughly from 2 to 6×10^6 (Fig. 1). At these realistic turbomachinery conditions with high Reynolds numbers, the calmed regions after wake passing, the laminar boundary layers and, particularly, the laminar separation bubbles will play a less important role.

Recent blade design and optimization studies by Köller et al. [8] and Küsters et al. [9] showed that under high free-stream turbulence levels, boundary layer transition on the blade suction side successively propagated forward into the accelerated front region

Contributed by the International Gas Turbine Institute and presented at the 45th International Gas Turbine and Aeroengine Congress and Exhibition, Munich, Germany, May 8–11, 2000. Manuscript received by the International Gas Turbine Institute February 2000. Paper No. 2000-GT-263. Review Chair: D. Ballal.

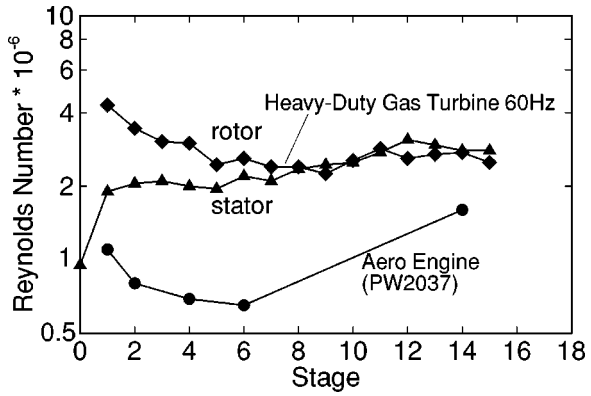

Fig. 1 Typical blade chord Reynolds number of a heavy-duty gas turbine compressor

of the blades when the Reynolds number was increased. The blade profile optimization algorithm employed considered this early transition location and set the velocity maximum on the blade suction side much further upstream than is common in so-called controlled diffusion designs, which assume at least partly laminar flow up to about 20–30 percent of chord [10]. It was clearly shown that the location of transition onset has a considerable influence on the blading design process. Conversely, the results of new blading designs depend strongly on the reliability of the transition models employed in the boundary layer codes. Therefore, it is essential that the transition models have been validated thoroughly for all turbomachinery relevant flow conditions with realistic turbulence levels and pressure gradients.

One correlation for transition onset, frequently used in numerical boundary layer codes and embedded in many design tools, is the correlation of Abu-Ghannam and Shaw [11]. It has been comprehensively verified for tests at lower turbulence levels for zero, adverse, and slightly favorable pressure gradients on flat plates. For high turbulence levels (>2 percent) there is little information and Gostelow and Bluden [12] emphasized that uncertainty exists for favorable gradients. Mayle [13] pointed out that, especially for favorable pressure gradients, there are only two data points from Blair [14] from a flat plate experiment with $Tu=2$ and 5 percent that give sufficient information on transition onset and length.

In this present study, experiments have been conducted in a linear cascade facility to give specific evidence that for higher turbulence levels and increasing Reynolds number, transition onset on real compressor blades moves upstream into the region of strong favorable pressure gradients. The test model used was a controlled diffusion airfoil with suction surface acceleration along a relatively long distance. This paper focuses on the investigation of the transition location for different levels of nearly *isotropic* turbulence and Reynolds numbers, a first step in which the complex mechanism of wake passing was neglected. The Reynolds number was increased beyond levels investigated so far. An oil flow technique and liquid crystal coatings have been used to visualize boundary layer state on the blade suction side.

Compressor Airfoil: Analytical Study

To study the effect of free-stream turbulence and Reynolds number on transition onset, a blade profile was selected that was designed for an inlet Mach number of 0.6 and a flow turning of 16 deg. Its profile pressure distribution is typical of controlled diffusion airfoils (CDA) with a favorable pressure gradient on the suction surface to 30 percent of chord and beyond the station of the maximum velocity, where the boundary layer is turbulent, a steep ''controlled diffusion'' with decreasing pressure gradient toward the trailing edge. Its profile Mach number distribution is shown in the upper part of Fig. 2.

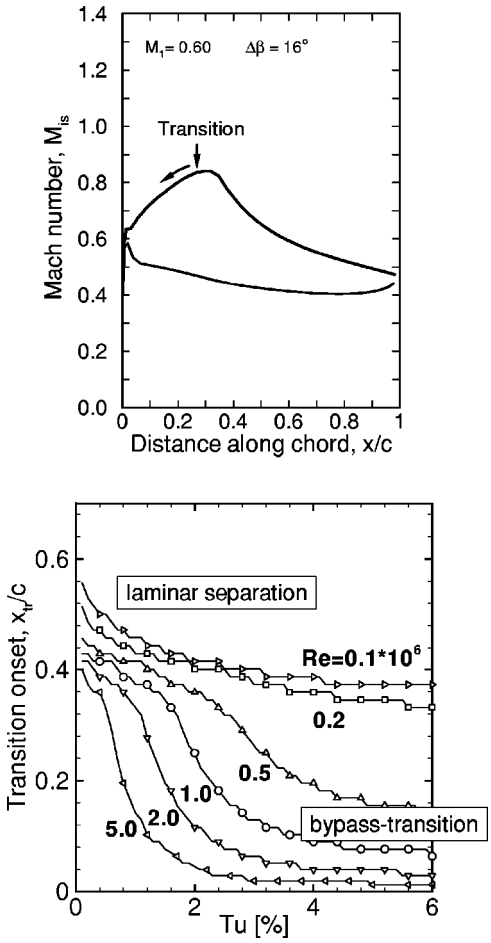

Fig. 2 Influence of Reynolds number and free-stream turbulence on suction side transition onset (MISES simulation)

The blade-to-blade solver MISES of Drela and Youngren [15] was used for the numerical study of boundary layer transition behavior. It is a coupled inviscid/viscous interaction method that employs integral boundary layer equations for boundary layer and wake development. Boundary layer transition is predicted employing the criterion of Abu-Ghannam/Shaw [11], which has been slightly modified by Drela [16] to achieve a more stable convergence during the coupling process.

Basically, transition can occur in three different modes; in a natural transition mode (Tollmien/Schlichting (TS) wave instabilities), in the ''bypass'' mode, or in the separated mode via a laminar separation bubble with turbulent reattachment. All these modes depend on the Reynolds number, the pressure gradient at the edge of the boundary layer, and the free-stream turbulence level. For high free-stream turbulence levels, transition primarily is induced from outside of the boundary layer and the stages of the natural transition process (TS instabilities) are ''bypassed''. For many practical flows TS wave transition and bypass transition both are often at work, but for favorable pressure gradients and higher turbulence levels, bypass transition is relevant exclusively.

For the present study, boundary layer transition is calculated for Reynolds numbers from 0.1 to 5×10^6 and different turbulence levels using the suction side Mach number distribution of Fig. 2. The results in Fig. 2 bottom show a tremendous influence on the suction side transition onset of both the Reynolds number and the turbulence level. For small turbulence levels ($Tu<1.5$ percent) and low Reynolds numbers, laminar separation is calculated after the velocity maximum and transition with turbulent reattachment is predicted to occur beyond 35 to 50 percent of chord. A stepwise

increase of the turbulence level up to 6 percent reduces the extent of the separation bubble, but as long as the Reynolds number does not exceed values of about 0.2×10^6, transition remains behind the velocity maximum ($x_t/c>0.3$). With increasing Reynolds numbers the bubble finally disappears and transition onset propagates upstream into the accelerated front portion of the blade. For example, at a Reynolds number of 2.0×10^6 and a turbulence level of 3 percent, transition onset is located near 6.1 percent of chord. Here the momentum thickness Reynolds number Re_θ, which is used as the criterion for transition onset, is calculated to be 220.

Overall, the curves in Fig. 2 illustrate that the transition onset location is most sensitive on the Reynolds number when the turbulence levels are between about 2 and 4 percent. Beyond $Tu=4$ percent the transition onset location for a given Reynolds number is more or less insensitive to higher Tu levels.

A further relevant influence parameter for boundary layer transition is the streamwise pressure gradient. Mayle [13] pointed out that for favorable pressure gradients, the flow acceleration parameter is the appropriate parameter to correlate transition onset

$$K=\frac{\nu}{U^2}\frac{dU}{ds}$$

To illustrate the acceleration rate on the blade surface of the present cascade, the calculated parameter K for the blade suction and pressure side is shown in Fig. 3. Calculations are presented for both a low and a high Reynolds number, the range in which the following experiments have been performed. On the front portion of the suction side this parameter exceeds values of 3 $\times10^{-6}$ but the value successively falls toward zero near the velocity maximum. According to the definition of the acceleration parameter, it is obvious that K is inversely proportional to the chord Reynolds number. Therefore, the magnitude of this parameter becomes smaller when the Reynolds number is increased. The correlation of the momentum thickness Reynolds number at transition onset against the acceleration parameter (Mayle [13], Fig. 16) claims that for free-stream turbulence levels beyond 3 percent, the acceleration parameter K has no influence on the momentum thickness Reynolds number $\mathrm{Re}_{\theta t}$. As there is little experimental information on transition with accelerated boundary layers ($K>0$) and high turbulence levels, the following experiments will provide further insight to this transition process and help to confirm or correct the transition correlation.

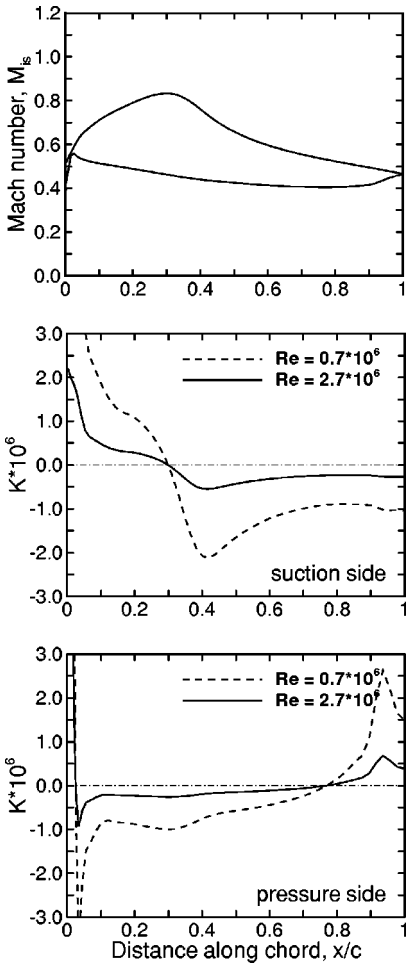

Fig. 3 Acceleration parameter for suction and pressure side for two different Reynolds numbers

Test Setup

The experiments were performed in the transonic cascade tunnel of the DLR Cologne [17]. This tunnel is a closed-loop, continuously running facility with a variable nozzle, an upper transonic wall, and a variable test section height. The air supply system enables an inlet Mach number range from 0.2 to 1.4 and a Mach number independent variation of the Reynolds number from about $1\times10^{*5}$ to $3\times10^{*6}$. Tunnel sidewall boundary layers ahead of the cascade are removed through protruding slots. Within the blade pack aft of the minimum pressure region, endwall boundary layers and AVDR are controlled by suction through chordwise slots. Tailboards combined with throttles are used to control inlet and exit boundary conditions.

To allow tests with high Reynolds numbers and to have a sufficient resolution of the blade surface, the cascade blade chord was enlarged to 150 mm. Three blades were installed in the test section, with the center blade instrumented on the pressure and suction side. A cross-sectional view of the test section and a photograph of the cascade model are shown in Figs. 4 and 5. For visualization tests using liquid crystal coating, the center blade was fabricated from a carbon-fiber-reinforced epoxy material to reduce a chordwise heat flux within the blade contour.

Most tests were run at an inlet Mach number of 0.6 with total pressures from 0.42 to 1.7 bar and total temperatures from about 306 to 310 Kelvin, giving blade chord Reynolds numbers from 0.7 to 2.8×10^6. Some tests at $M_1=0.7$ allowed Reynolds numbers around $3\times10^{*6}$. To increase the turbulence level, three different turbulence grids constructed from rectangular bars were installed near the entrance to the main tunnel contraction, one about 1.9 m and an even more coarse grid 1.55 m upstream of the test section.

Experimental Results

Two main test series with different turbulence levels have been performed: The first one used a standard oil flow technique and the second one employed liquid crystal coatings. The minimum

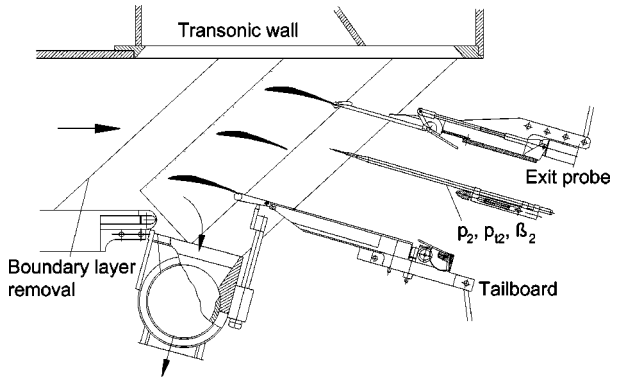

Fig. 4 Test section of the DLR Transonic Cascade Tunnel

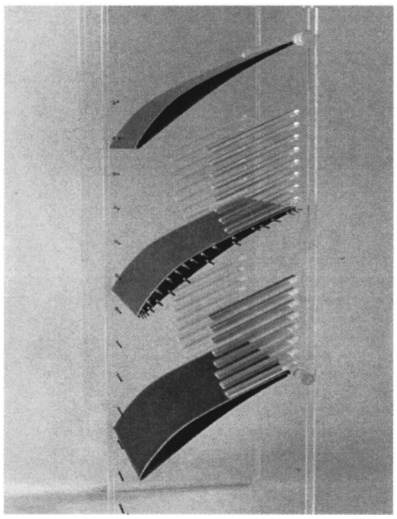

Fig. 5 Photograph of cascade and endwalls

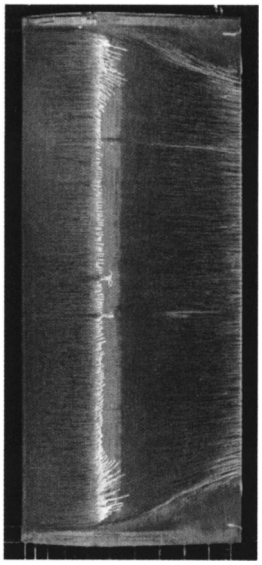

Fig. 6 Oil streak lines on suction side, $M_1=0.6$, $Re=0.8\times10^6$

turbulence level without a grid installed was measured to be 0.7 percent. Two grids were located near the entrance of the tunnel contraction; the first one, denoted ''screen 1.9'' with rectangular bars of about 20 mm, generated a turbulence level of about 2.5–3 percent and the second one, ''screen 1.9+4,'' had bars of 20 mm with four additional bars of 6 mm, generated slightly higher frequencies.

During the course of the investigations it turned out that the turbulence level of the first two grids was not sufficient to induce the expected upstream propagation of transition onset. Therefore, an even coarser grid (''screen 2.6'' with 25 mm bars) was located slightly closer to the test blade, generating a turbulence level of about 4–5 percent.

Oil Flow Visualization. In a preceding test series with blades of 70 mm chord an oil flow picture (Fig. 6) was obtained at a low Reynolds number of 0.8×10^6 and a turbulence level of 0.7 percent (no grid installed). Figure 6 shows the oil traces on this blade, which had an aspect ratio of 2.4. Due to a distinct suction side velocity maximum around 30 percent of chord, which is followed by a relatively strong diffusion, the laminar separation is well developed and establishes as a short bubble between about 34 to 41 percent.

All further experiments presented here were performed using a blade chord of 150 mm. Keeping the Reynolds number at the same low level (0.7×10^6) as in Fig. 6, but increasing the turbulence level, the laminar separation behavior does not change considerably. The blade Mach number distribution and the oil traces in Fig. 7 both again indicate a separation bubble for a *Tu* level of 2.5 percent and a Reynolds number of 0.7×10^6. This separation bubble, however, disappeared when the Reynolds number was increased to $Re=2.0\times10^6$. At this high Reynolds number and *Tu* level the oil traces do not show a specific change of their structure along the blade suction side (Fig. 8). Obviously, the discontinuity in c_f is not sufficiently distinct to show an essential difference on the blade surface, at least downstream of about 15 percent of chord. As at high Reynolds numbers the boundary layer is thinner, the measured total pressure losses are lower compared to those of the low Reynolds number tests and the experimental blade Mach number distribution does not show the separation bubble. A numerical simulation employing the blade to blade solver MISES nearly exactly matches the measured surface Mach number distribution, as shown in Fig. 8.

Further high Reynolds number tests with oil flow visualization and even higher turbulence levels ($Tu=4-5$ percent) did not provide a clear c_f-induced change in the surface flow structure within

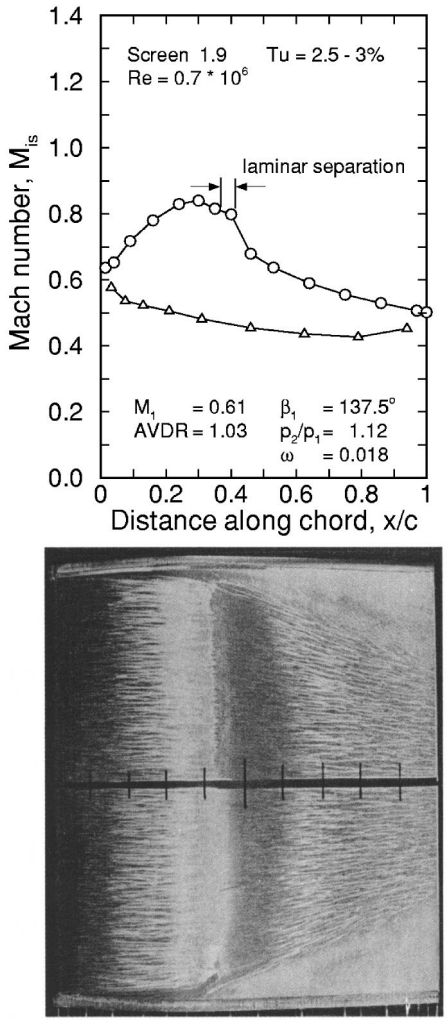

Fig. 7 Mach number distribution and oil streak lines at Re $=0.7\times10^6$ and $Tu\approx2.5-3$ percent, 1 tick approximately 10 percent of chord

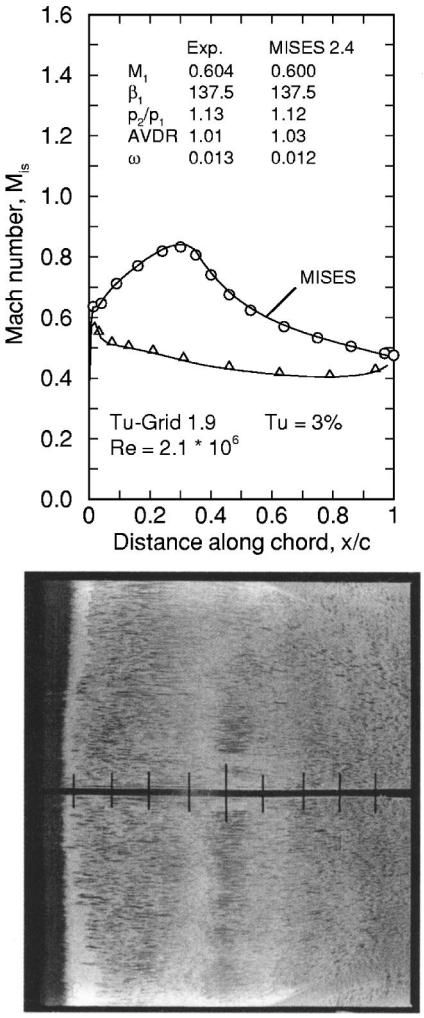

Fig. 8 Mach number distribution and oil streak lines at Re $=2.1\times10^6$ and $Tu\approx3$ percent, 1 tick approximately 10 percent of chord

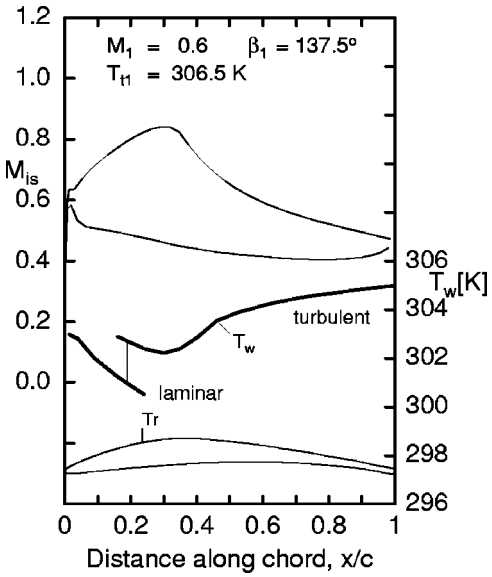

Fig. 9 Predicted blade Mach number distribution and calculated adiabatic wall temperature on suction side

the accelerated front portion of the blade and thus no evidence regarding transition in this region. Therefore, the tests have been repeated using sensitive liquid crystal coatings.

Visualization Using Liquid Crystal Coatings. Liquid crystal coatings have been used to detect transition by visualizing the difference in adiabatic wall temperature between laminar and turbulent boundary layers. This technique requires a relatively sensitive mixture of liquid crystals that is sprayed on the black colored blade surface. To achieve a sufficient contrast in wall temperature as reflected through colors of the liquid crystals, it was necessary to use a thermally insulated test blade that was made completely out of carbon fiber composite. The event temperature of the liquid crystals is selected to be approximately 4–5°C lower than the total temperature and within the sensitive temperature range (about 2°C) the colors of the scattered light are red, yellow, and green. Before approaching this range the liquid crystals are transparent and the blade surface looks black. A fine tuning of the total temperature in steps of about 0.1 deg allows an adjustment of the wall temperature to the event temperature of the liquid crystals (303–305 K). More information on this visualization technique is given in a previous report by Steinert and Starken [18] and a recent measurement technique paper by Bize et al. [19] for example.

The adiabatic surface temperature T_w, which depends on the type of boundary layer and the Mach number at the boundary layer edge, is calculated for the present cascade from its surface Mach number distribution using the different recovery factors for laminar and turbulent flow ($r=0.836$ and 0.89, respectively). Figure 9 shows that in the front portion of the suction side a maximum temperature difference of about 2 K can be expected between laminar and turbulent flow. Prior to the tests, a numerical parameter study was performed for a high Reynolds number and four different turbulence levels to estimate the expected location and magnitude of the temperature difference across transition. The model used for prediction of transition again was the modified correlation of Abu-Ghannam and Shaw [16]. Figure 10 shows the calculated suction side temperatures for the tests at the Reynolds number of $2.6\times10^6$and turbulence levels from 0.5 to 3 percent. The highest temperature difference across transition can be expected for the low turbulence level test. That case results in the lowest temperatures for the laminar flow at velocity maximum and a theoretical temperature increase of more than 2 K near 40

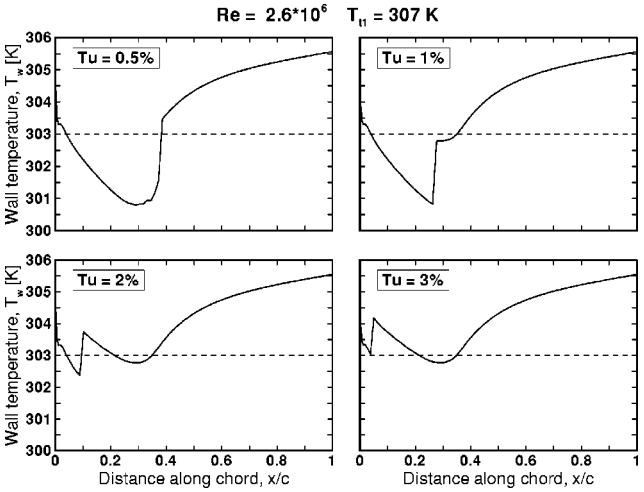

Fig. 10 Simulated surface temperature distribution on blade suction side, influence of free-stream turbulence on temperature discontinuity near transition for $M_1=0.6$ and $Re=2.6\times10^6$

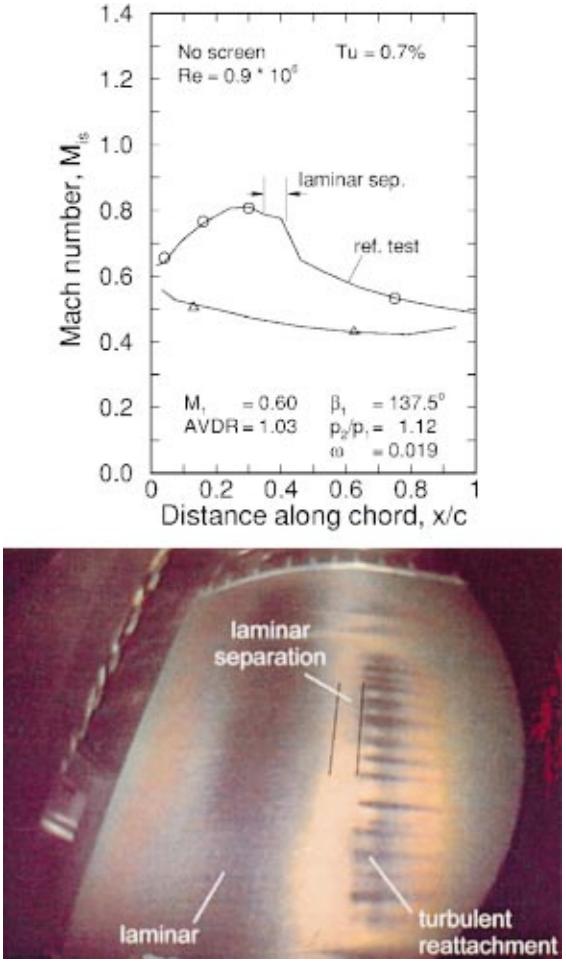

Fig. 11 Mach number distribution and liquid crystal picture of suction side at Re=0.9×10^6 and *Tu*≈0.7 percent showing laminar separation and turbulent reattachment

percent of chord. When transition propagates upstream with increasing *Tu* levels, this temperature difference unfortunately becomes somewhat less.

As transition in reality is a three-dimensional and more gradual process, the temperature increase on the surface will not be as pronounced and clear as predicted in Fig. 10, especially for the high-turbulence-level tests. The transition-induced change in surface temperature for those conditions, however, is still more pronounced than the gradual temperature variation that is caused by the local change of the surface Mach number. Certainly, some uncertainty remains concerning the precise experimental determination of the transition location. The theory (with $Tu=3$ percent) would expect early transition within the accelerated front portion around 5 percent of chord. The position of laminar separation and reattachment from the experiment, however, is quite accurate.

The first test presented in Fig. 11 shows a low-Reynolds-number test without a turbulence grid upstream ($Tu\approx0.7$ percent). Black regions in the blade front portion indicate a cold laminar boundary layer. The ''warm'' laminar separation bubble to be seen between 34 and 41 percent of chord, is yellow-red followed by a streaky ''partly cold'' turbulent reattachment zone. Evidently, turbulent reattachment takes place in combination with longitudinal vortices, which produce a streaky temperature distribution. The rear turbulent blade surface shows increasing temperatures with yellow-red-green colors. Similar observations at such low Reynolds number tests had been shown previously by Steinert and Starken [18].

When increasing the Reynolds number to about 2.2×10^6 but keeping the turbulence level as low as before (no turbulence grid), the liquid crystal picture again showed laminar flow in the front portion; the yellow stripe, that indicates laminar separation, practically disappeared, but again or still, the streaky turbulent ''reattachment zone'' remained (Fig. 12). The blade Mach number distribution in Fig. 12 (top) provides no clear indication for a laminar separation bubble. Due to the increased Reynolds number, the thinner boundary layer now starts to become sensitive to certain roughness particles. Therefore, first yellow ''turbulence wedges,'' located downstream of isolated small grains or excrescencies, become visible within the laminar front portion.

Increasing the turbulence level to about 2.5 percent, one sees the weak laminar separation bubble completely disappears and boundary layer transition starts around 30 percent of chord, i.e., near the suction side velocity maximum (Fig. 13). A slightly higher turbulence level ($Tu\approx3$ percent) provides only a marginal upstream shift of transition and the liquid crystal picture in Fig. 14 does not confirm the forward transition location that was predicted by the MISES code near 5 percent of chord (see Fig. 2 or for a similar condition Fig. 10 bottom right). However, the number of roughness-induced turbulence wedges increases considerably so that wide areas of the laminar flow effectively become turbulent. On the other hand, these turbulence wedges provide a clear evidence that the suction surface flow beside these wedges is *laminar.*

A final upstream movement of the transition process could be achieved only with a coarser turbulence grid. At about 4–5 percent turbulence intensity the bypass mechanism becomes dominant, and transition is observed upstream of 10 percent of chord (Fig. 15). A test with an even more increased Reynolds number could be achieved at an inlet Mach number of 0.7. Figure 16 provides the liquid crystal visualization for a Reynolds number of 3.1×10^6 and a turbulence level of about 3.5 percent generated by the turbulence grid denoted ''screen 1.9+4.'' About 70 percent of the blade front portion is covered with turbulence wedges, revealing the increasing sensitivity to surface roughness.

A comparison of the transition locations derived from the visualization experiments to the predicted locations, employing the criterion of the MISES code [16], is shown in Fig. 17 for a constant Reynolds number of 2×10^6. Overall, the forward movement of transition onset with rising turbulence level can be confirmed qualitatively; but around $Tu=3$ percent the Abu-Ghannam and Shaw/Drela correlation slightly overpredicts the forward movement of transition into the accelerated blade front portion. Some uncertainties remain because within the domain of higher Reynolds numbers surface roughness seems to play an additional, but essential, role.

Surface Roughness

The foregoing observations clearly show that both free-stream turbulence and surface roughness have a considerable influence on transition. At low Reynolds numbers, roughness is relatively harmless, but the boundary layer becomes very sensitive when the Reynolds number is increased. The test blade, which is covered with liquid crystals, has a certain roughness that probably could induce premature transition before the bypass transition process becomes dominant. To ensure that the surface roughness remains below the critical roughness height and that the global spanwise transition onset either is natural transition or really is induced by free-stream turbulence, a theoretical estimation was performed, the results of which are presented in Fig. 18. This figure, derived from a diagram in Mayle [13], presents a correlation of the momentum thickness Reynolds number at the onset of transition plotted against a roughness parameter (from Mick [20], upper dashed-dotted line). If Re_θ lies above this curve, surface roughness would induce transition. The nearly straight lines in Fig. 18 represent calculated Re_θ developments along the blade surface of the

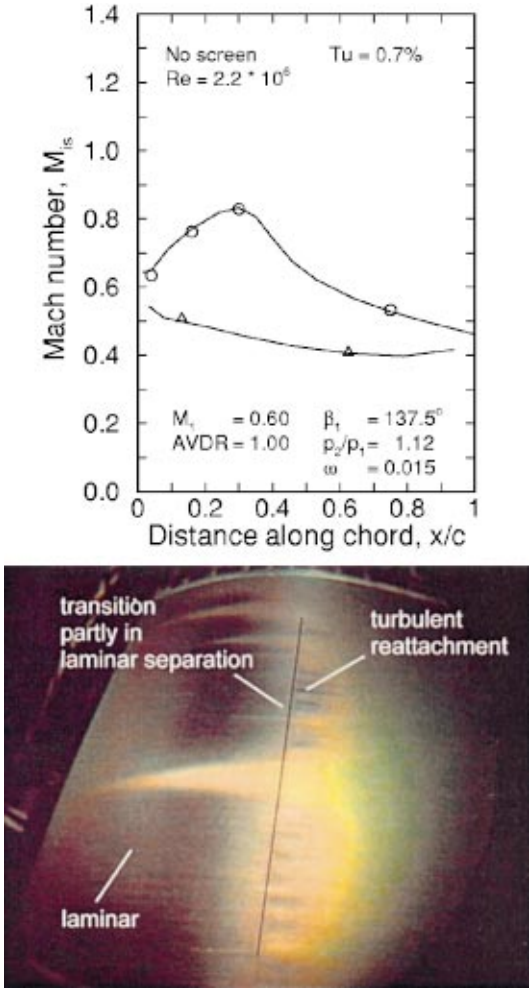

Fig. 12 Mach number distribution and liquid crystal picture of suction surface at Re=2.2×10⁶ and *Tu*≈0.7 percent (no screen)

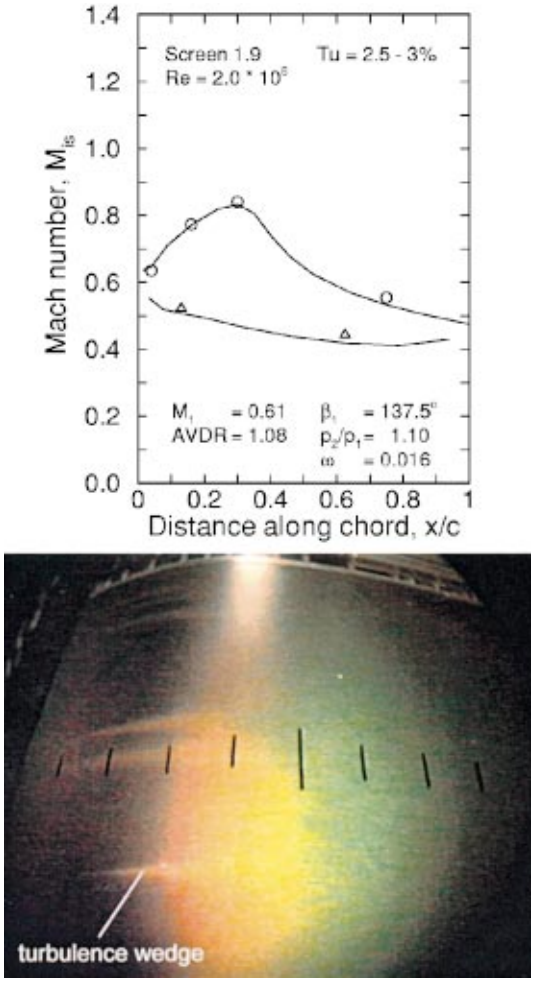

Fig. 13 Mach number distribution and liquid crystal picture of suction surface at Re=2.0×10⁶ and *Tu*≈2.5–3 percent (screen 1.9)

present cascade for sand roughness heights of 5, 10, and 20 μm. Roughness measurements of the tested blade surface yielded sand roughness heights not greater than $k_s = 10$ μm (with $k_s = 8.6 \times Ra$, following Schäffler [21]). As the curve with $k_s = 10$ μm does not intersect the limiting curve for Re_θ transition, it can be concluded, or at least suspected, that transition at the high Reynolds numbers and high turbulence level is bypass transition, and not roughness, induced transition.

A further interesting and essential finding of these visualization experiments can be seen in Figs. 12–15. These figures again show

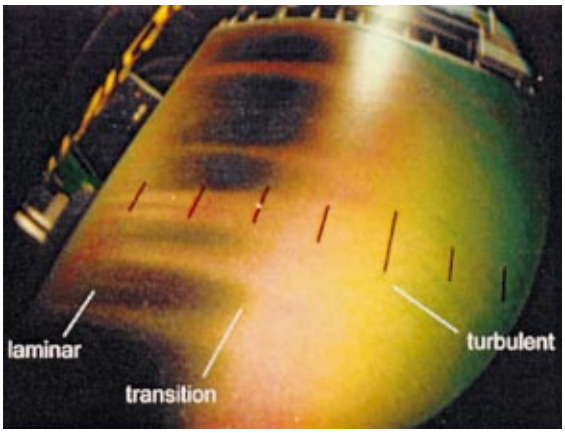

Fig. 14 Liquid crystal picture of suction surface at Re=2.0×10⁶ and *Tu*≈3–3.5 percent (screen 1.9+4)

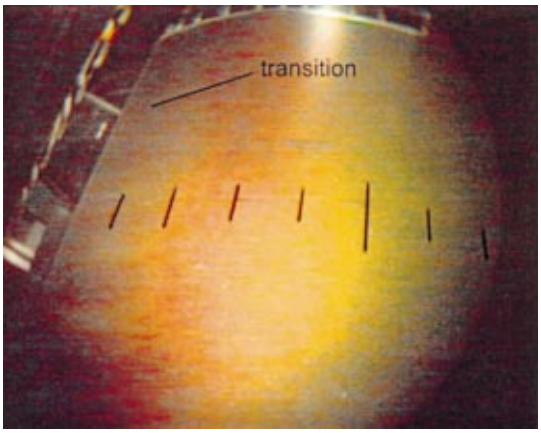

Fig. 15 Liquid crystal picture of suction surface at Re≈2.0×10⁶ and *Tu*≈4–5 percent (screen 2.6)

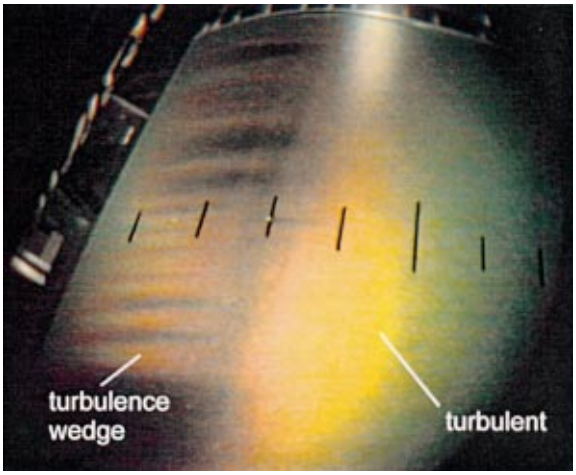

Fig. 16 Liquid crystal picture of suction surface at $M_1=0.7$, $Re=3.1\times10^6$ and $Tu\approx3-3.5$ percent

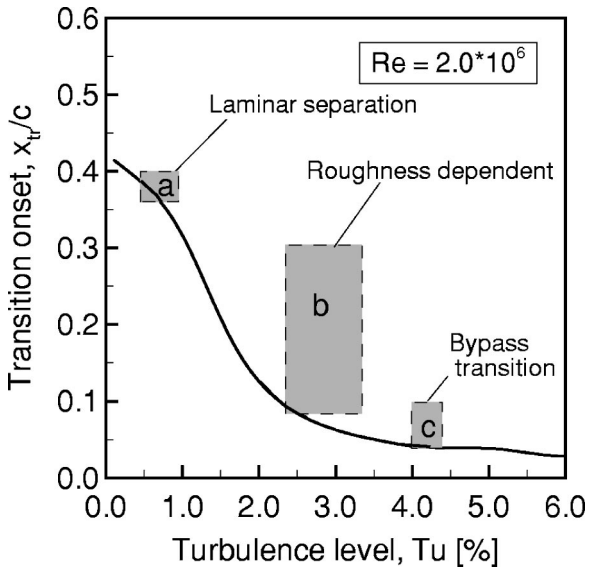

Fig. 17 Experimental (shaded area) and predicted (solid line) suction side transition onset at $Re=2\times10^6$

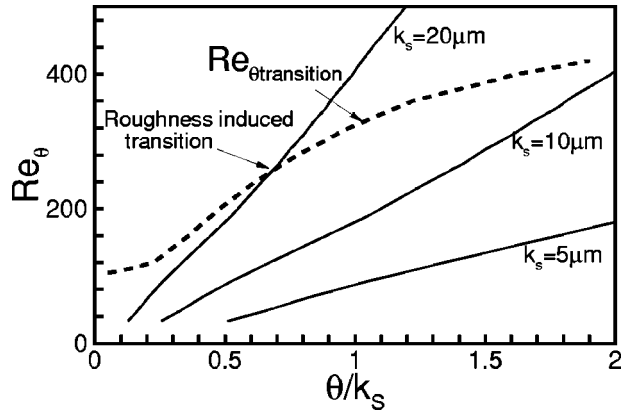

Fig. 18 Momentum thickness Reynolds number Re_θ calculated for three different roughness heights in comparison to Re_θ transition (dashed line from [20]) against the roughness parameter θ/k_s

tests for increasing turbulence levels at a high, but practically constant, Reynolds number of 2×10^6. As the turbulence level was raised, more and more turbulence wedges on the blade surface become visible originating with small roughness particles. Evidently, the particles alone are not able to produce turbulence, but the interaction of the particle-induced instabilities inside the boundary layer with disturbances of sufficient strength from the outer free-stream turbulence seems to initiate turbulence in the boundary layer. This interaction of surface particle-induced instabilities with the disturbances coming from outside of the boundary layer is a complex, but rather important, mechanism that must be considered in future research work on transition onset.

Conclusions

Surface flow visualization tests have been performed on the blade suction side of a controlled diffusion compressor blade to show the effect of Reynolds number and free-stream turbulence on transition location. At the low Reynolds number of 0.8×10^6, a clear laminar separation bubble with turbulent reattachment is visible on the suction side, which does not disappear when free-stream turbulence is increased to 3 percent.

The main focus, however, was on suction side transition onset at high Reynolds number ($Re>2\times10^6$) and accelerated boundary layers ($K>0$). A numerical study employing a modified Abu-Ghannam and Shaw correlation indicated that for high Reynolds numbers and an increasing turbulence level ($Tu\geqslant3$ percent), transition propagates far forward into the accelerated region of the suction side. The experiments qualitatively confirmed an upstream movement of transition, but a slightly higher *Tu* level was necessary to induce early bypass transition. Additionally, the tests clearly showed, that besides both increasing Reynolds number and turbulence level, the *surface roughness* plays an essential role. At high Reynolds numbers, roughness-induced turbulence wedges cover wide areas of the blade front portion so that laminar flow has a less important influence.

The results of both the numerical study and experiment suggest that for high Reynolds numbers, blading design has to consider the effect of early transition onset. Compressor blades with a transition location shortly after the blade leading edge should obtain a front-loaded blade pressure distribution at least for subsonic flows with a forward-located suction side velocity maximum.

When considering the more complex unsteady effects of wake-blade boundary layer interaction, one should consider that for high Reynolds numbers, laminar boundary layers are less important, and that the calming effects after wake-induced transition may be altered considerably. Furthermore, the combined effect of surface roughness at high Reynolds numbers and high turbulence level is an important field for future research work on boundary layer development in turbomachinery blading.

Nomenclature

AVDR = axial velocity density ratio $=(\rho_2 w_2 \sin\beta_2)/(\rho_1 w_1 \sin\beta_1)$
k_s = height of standard sand roughness, μm
K = acceleration parameter $\nu/U^2*(dU/ds)$
M = Mach number
M_{is} = isentropic Mach number $=f(p/p_{t1})$
Ra = arithmetic average roughness
Re = Reynolds number $=u_1 c/\nu_1$
T = temperature
T_W = adiabatic wall temperature
Tu = turbulence level
c = profile chord length
p = pressure
s = blade spacing, pitch
U = velocity at edge of boundary layer
u = velocity
β = flow angle with respect to cascade front

$\Delta\beta$ = flow turning $= \beta_1 - \beta_2$
ν = kinematic viscosity
ρ = density
ω = total pressure loss coefficient $= (p_{t1} - p_{t2})/(p_{t1} - p_1)$
θ = boundary layer momentum thickness

Subscripts

1 = inlet plane
2 = exit plane
is = isentropic entity
t = total, stagnation value
t = transition

References

[1] Dong, Y., and Cumptsy, N., 1990, ''Compressor Blade Boundary Layers: Part 2—Measurements With Incident Wakes,'' ASME J. Turbomach., **112**, pp. 231–240.

[2] Teusch, R., Fottner, L., and Swoboda, M., 1999, ''Experimental Investigation of Wake-Induced Transition in a Linear Compressor Cascade With Controlled Diffusion Blading,'' 14th ISABE Conference, Florence, Sept., Paper No. 99-7057.

[3] Solomon, W. J., and Walker, G. J., 1995, ''Observation of Wake-Induced Transition on an Axial Compressor Blade,'' ASME Paper No. 95-GT-381.

[4] Halstead, D. E., Wisler, D. C., Okiishi, T. H., Walker, G. J., Hodson, H. P., and Shin, H. W., 1997, ''Boundary Layer Development in Axial Compressors and Turbines: Part 1–4,'' ASME J. Turbomach., **119**, pp. 114–127; 426–444; 225–237; 128–139.

[5] Pieper, S., Schulte, J., Hoynacki, A., and Gallus, H.E., 1996, ''Experimental Investigation of a Single Stage Axial Flow Compressor With Controlled Diffusion Airfoils,'' ASME Paper No. 96-GT- 81.

[6] Cumpsty, N. A., Dong, Y., and Li, Y. S., 1995, ''Compressor Blade Boundary Layers in the Presence of Wakes,'' ASME Paper No. 95- GT-443.

[7] Hourmouziadis, J., 1989, ''Aerodynamic Design of Low Pressure Turbines,'' AGARD Lecture Series No. 167.

[8] Köller, U., Mönig, R., Küsters, B., and Schreiber, H. A., 2000, ''Development of Advanced Compressor Airfoils for Heavy-Duty Gas Turbines, Part I: Design and Optimization,'' ASME J. Turbomach., **122**, pp. 397–405.

[9] Küsters, B., Schreiber, H. A., Köller, U., and Mönig, R., 1999, ''Development of Advanced Compressor Airfoils for Heavy Duty Gas Turbines, Part II: Experimental and Analytical Analysis,'' ASME J. Turbomach., **122**, pp. 406–414.

[10] Wisler, D. C., 1985, ''Loss Reduction in Axial-Flow Compressors Through Low Speed Model Testing,'' ASME J. Eng. Gas Turbines Power, **107**, pp. 354–363.

[11] Abu-Ghannam, B. J., and Shaw, R., 1980, ''Natural Transition of Boundary Layers—The Effect of Turbulence, Pressure Gradient and Flow History,'' J. Mech. Eng. Sci., **22**, No. 5, pp. 213–228.

[12] Gostelow, J. P., and Bluden, A. R., 1989, ''Investigation of Boundary Layer Transition in an Adverse Pressure Gradient,'' ASME J. Turbomach., **111**, pp. 366–375.

[13] Mayle, R. E., 1991, ''The 1991 GTI Scholar Lecture: The Role of Laminar–Turbulent Transition in Gas Turbine Engines,'' ASME J. Turbomach., **113**, pp. 509–537.

[14] Blair, M. F., 1982, ''Influence of Free-Stream Turbulence on Boundary Layer Transition in Favorable Pressure Gradients,'' ASME J. Eng. Power, **104**, pp. 743–750.

[15] Drela, M., and Youngren, H., 1991, ''Viscous/Inviscid Method for Preliminary Design of Transonic Cascades,'' AIAA Paper No. 91-2364.

[16] Drela, M., 1995, ''Implementation of Modified Abu-Ghannam Shaw Transition Criterion,'' MISES User's Guide, MIT, Computational Aerospace Science Lab., Cambridge, MA.

[17] Schreiber, H. A., Starken, H., and Steinert, W., 1993, ''Transonic and Supersonic Cascades,'' AGARDOgraph ''Advanced Methods for Cascade Testing,'' AGARD AG 328, pp. 35–59.

[18] Steinert, W., and Starken, H., 1996, ''Off-Design Transition and Separation Behavior of a CDA Cascade,'' ASME J. Turbomach., **118**, pp. 204–210.

[19] Bize, D., Lempereur, C., Mathe, J. M., Mignosi, A., Seraudie, A., and Serrot, G., 1998, ''Transition Analysis by Surface Temperature Mapping Using Liquid Crystals,'' Aerospace Sci. Tech., Paris, No. 7, pp. 439–449.

[20] Mick, W. J., 1987, ''Transition and Heat Transfer in Highly Accelerated Rough-Wall Boundary Layers,'' Ph.D. Thesis, Rensselaer Polytechnic Institute, Troy, NY.

[21] Schäffler, A., 1980, ''Experimental and Analytical Investigation of the Effect of Reynolds Number and Blade Surface Roughness on Multistage Axial Flow Compressors,'' ASME J. Eng. Power, **102**, pp. 5–12.